Available online at www.sciencedirect.com
ScienceDirect
International Journal of Heat and Mass Transfer 51 (2008) 4563–4572
International Journal of HEAT and MASS TRANSFER
www.elsevier.com/locate/ijhmt

Analytical solution of combined heat and mass transfer performance in a cross-flow packed bed liquid desiccant air dehumidifier

Xiao-Hua Liu *, Yi Jiang, Kai-Yang Qu

Department of Building Science, School of Architecture, Tsinghua University, Beijing 100084, PR China

Received 12 October 2005; received in revised form 20 July 2006
Available online 12 April 2008

Abstract

Heat and mass transfer between air and liquid desiccant in a cross-flow packed bed dehumidifier is investigated. Analytical solutions of air and desiccant parameters as well as enthalpy and moisture efficiencies are given in the present study, based on the analogy between the combined heat and mass transfer process in the cross-flow dehumidifier and the heat transfer process in the cross-flow heat exchanger. The results given by the analytical solution are compared with numerical solutions and experimental findings. Good agreement is shown between the analytical solutions and the numerical or experimental results. The analytical solutions can be used in the optimization of the cross-flow dehumidifier.

Keywords: Liquid desiccant; Cross-flow dehumidifier; Analytical solution; Optimization

1. Introduction

Temperature and humidity are two essentially important factors in air-conditioning system. In conventional air-conditioning systems, dehumidification is realized by cooling down air below its dew point, which would lower the COP of chillers since relatively lower temperature 7/12 °C chilled water is required. Sometimes the processed dry air has to be reheated before being supplied to the occupied space; therefore more energy is required to reheat the air to a comfortable temperature. Furthermore, it is easier to cause health problems, for the condensed water makes the coil surface as a hot-bed for bacteria. Liquid desiccant air-conditioning system seems to be a recommended dehumidification method to avoid such problems [1–3]. Liquid desiccant system can be driven by low grade energy, has the advantages in removing the latent load and possible bactericidal effect.

The dehumidifier is one of the most important components in the liquid desiccant system, whose heat and mass transfer performance directly affect the whole system performance. In the dehumidifier, combined heat and mass transfer processes occur synchronously, and heat transfer and mass transfer process influence each other. Moisture is transferred from the humid air to the liquid desiccant in the dehumidifier due to the vapor pressure difference between the air and the desiccant, while vaporization latent heat is released during the mass transfer process. The increase in air and desiccant temperature results in not only the changes of heat transfer process, but also the decrease of the mass transfer driving potential since vapor pressure of the liquid desiccant increases remarkably with increasing desiccant temperature.

Many researchers have built up theoretical models for the combined heat and mass transfer process in the packed type dehumidifier, such as Factor and Grossman [4], Gandhidasan et al. [5,6], Stevens et al. [7], Rocha et al. [8] for counter-flow packed dehumidifiers, Lu et al. [9], Liu et al. [10] and Dai and Zhang [11] for cross-flow packed bed dehumidifiers. In packed bed dehumidifiers, air and liquid desiccant exchange heat and moisture adiabatically. The heat released during the dehumidification will increase the desiccant temperature, thus

* Corresponding author. Tel.: +86 10 6277 3772; fax: +86 10 6277 0544.
E-mail address: lxh@mail.tsinghua.edu.cn (X.-H. Liu).

0017-9310/$ - see front matter © 2008 Elsevier Ltd. All rights reserved.
doi:10.1016/j.ijheatmasstransfer.2007.11.059

Nomenclature

a	specific area of packing per volume (m^2/m^3)
A	overall heat (and mass) transfer areas (m^2)
X	concentration of the liquid desiccant (%)
c_p	specific heat (kJ/kg °C)
d_e	equivalent diameter of the packing (m)
D	diffusion coefficient (m^2/s)
F	sectional mass flow rate (kg/m^2 s)
H	height of the cross-flow dehumidifier/heat exchanger (m)
h	enthalpy (kJ/kg)
L	thickness of the cross-flow dehumidifier/ heat exchanger (m)
Le	Lewis number (dimensionless)
m^*	thermal capacity ratio of air to desiccant (dimensionless)
$\dot{m}$	mass flow rate (kg/s)
NTU	number of transfer unit (dimensionless)
r_t	vaporization latent heat at the temperature of t (kJ/kg)
Re	Reynolds number (dimensionless)
Sc	Schmidt number (dimensionless)
Sh	Sherwood number (dimensionless)
t	temperature (°C)
v	surface velocity (m/s)
V	packing volume (m^3)
W	width of the cross-flow dehumidifier/ heat exchanger (m)

Greek symbols

α	heat transfer coefficient (kW/m^2 °C)
α_m	mass transfer coefficient (kg/m^2 s)
γ	dimensionless humidity ratio defined in Eq. (30) (dimensionless)
ε_h	enthalpy efficiency (%)
ε_m	moisture (or dehumidification) efficiency (%)
ζ	dimensionless enthalpy defined in Eq. (24) (dimensionless)
κ	difference of air inlet parameter to inlet desiccant isoconcentration line (dimensionless)
ω	humidity ratio of humid air (kg/kg)
Δp	pressure drop (Pa)
Δp^*	pressure drop per unit thickness (Pa/m)

Subscripts

a	air
e	equilibrium status of air with liquid desiccant
s	liquid desiccant
in	inlet
out	outlet
0	original condition

decrease the desiccant absorption ability. While in falling film type dehumidifier, the released latent heat can be carried over by the extra cooling source, such as in the study of Ali et al. [12,13], the wall temperature is fixed as 10 °C during the dehumidification process. The parametric study is employed to analyze the main controlling parameters on the dehumidification process. Such as in the cross-flow falling film type dehumidifier [13], it is found that an increase in the height and length of the channel and a decrease in the channel width will enhance the dehumidification and cooling capabilities. The internally cooled falling film dehumidifier may have higher effectiveness than the packed bed adiabatic dehumidifier, yet the manufacture process will be more difficult compared to the packed type, hence present study still focuses on the packed bed dehumidifier.

Finite-difference models [4–10] are usually taken in the analysis of packed bed dehumidifiers, in which the assumption of slug flows of air and desiccant flows separated by the heat and mass transfer surface is usually adopted. Most of the theoretical models were solved by numerical simulation, except that Stevens et al. [7] for counter-flow packed bed dehumidifier and Lu et al. [9] for cross-flow dehumidifier. In the study of Lu et al. [9], the air and desiccant are assumed mixed breadthwise in cross-flow dehumidifier, which is simplified as one-dimensional process. However, air and desiccant parameters change not only in the flow direction but also the transverse direction in most operation conditions, the analytical solutions are limited in the applications. The analytical solutions can be easily used to analyze the influencing factors of the combined heat and mass transfer performances in the dehumidifier, and helpful in the optimization of liquid desiccant air-conditioning systems. Yet, almost no report on analytical solution for cross-flow dehumidifier, in which air and desiccant are not mixed breadthwise, can be found in the available literature, since the complexity of the dehumidifier configuration.

Based on the previous combined heat and mass transfer theoretical model, some reasonable assumptions are adopted to simplify the model in the present study. Analytical solutions of air and desiccant parameters as well as heat and mass transfer efficiencies in cross-flow packed bed dehumidifier are derived, according to the analogy with cross-flow heat exchanger. The numerical results and experimental findings are used to validate the analytical solutions. The analytical solutions are then used to optimize the cross-flow dehumidifier.

2. Theoretical model

2.1. Control equations

The schematic of the cross-flow packed bed dehumidifier is shown in Fig. 1a, with the height, thickness and width of H, L and W, respectively. Random or structural packing is placed inside the dehumidifier to enlarge the heat and mass transfer area between the air and liquid desiccant. The liquid desiccant flows from the top and air is introduced into the dehumidifier from the left. The heat and mass transfer performances can be simplified as two-dimensional problem, as shown in Fig. 1b, when the air and liquid desiccant coming into the dehumidifier uniformly.

In the finite-difference model, uniform heat and mass transfer coefficients are assumed. The detailed mathematical model for cross-flow packed bed dehumidifier is described in a former paper [10], only the main equations are listed here. The energy balance and mass balance equations are shown in Eqs. (1) and (2) respectively for the cross-flow dehumidifier. Where, $\dot{m}$ is mass flow rate, h is enthalpy, subscripts a and s stands for air and liquid desiccant, respectively:

$$\frac{\dot{m}_a}{H}\cdot\frac{\partial h_a}{\partial z}+\frac{1}{L}\cdot\frac{\partial(\dot{m}_s h_s)}{\partial x}=0, \tag{1}$$

$$\frac{\dot{m}_a}{H}\cdot\frac{\partial \omega_a}{\partial z}+\frac{1}{L}\cdot\frac{\partial \dot{m}_s}{\partial x}=0. \tag{2}$$

The combined heat and mass transfer and moisture transfer between the air and desiccant are shown as follows, where α and α_m are heat transfer coefficient and mass transfer coefficient, respectively:

$$\dot{m}_a\frac{\partial h_a}{\partial z}=\frac{\alpha A}{L}(t_s-t_a)+r_{t_s}\dot{m}_a\frac{\partial \omega_a}{\partial z}, \tag{3}$$

$$\dot{m}_a\frac{\partial \omega_a}{\partial z}=\frac{\alpha_m A}{L}(\omega_e-\omega_a). \tag{4}$$

Combine Eqs. (3) and (4) to gain:

$$\frac{\partial h_a}{\partial z}=-\frac{\mathrm{NTU}\cdot Le}{L}\cdot\left[(h_a-h_e)+\left(\frac{1}{Le}-1\right)\cdot(\omega_a-\omega_e)\cdot r_{t_s}\right] \tag{5}$$

$$\frac{\partial \omega_a}{\partial z}=-\frac{\mathrm{NTU}}{L}\cdot(\omega_a-\omega_e) \tag{6}$$

ω_e and h_e is the humidity ratio and enthalpy, respectively, of air in equilibrium with liquid desiccant. Le and NTU [7,9,10] in the above equations are defined as, where $c_{p,m}$ is the specific heat of the humid air:

$$Le=\frac{\alpha}{\alpha_m c_{p,m}}, \tag{7}$$

$$\mathrm{NTU}=\frac{\alpha_m\cdot A}{\dot{m}_a}. \tag{8}$$

Eqs. (1), (2), (5) and (6) are the fundamental control equations for the combined heat and mass transfer performances in the cross-flow dehumidifier. Fig. 2 gives the relationship between the mass transfer process and the heat transfer process. The left side of the dividing line stands for the heat transfer process, and the right side stands for the mass transfer process. There are two lines go through the dividing line: one line is the impact of desiccant temperature on desiccant vapor pressure or ω_e, which embodies the influence of heat transfer performance on the mass transfer process; and another line is the latent heat released or absorbed during the mass transfer process, which affects the influence of mass transfer performance on heat transfer process.

2.2. Simplification of the control equations

The assumptions used in the following analysis is that the moisture content absorbed by the liquid desiccant during the dehumidification process can be neglected compared with the desiccant mass flow rate, which is verified by lots of experimental results [14–16]. Therefore, constant liquid desiccant mass flow rate and constant concentration within the dehumidifier can be easily gained. Eq. (1) can be rewritten as

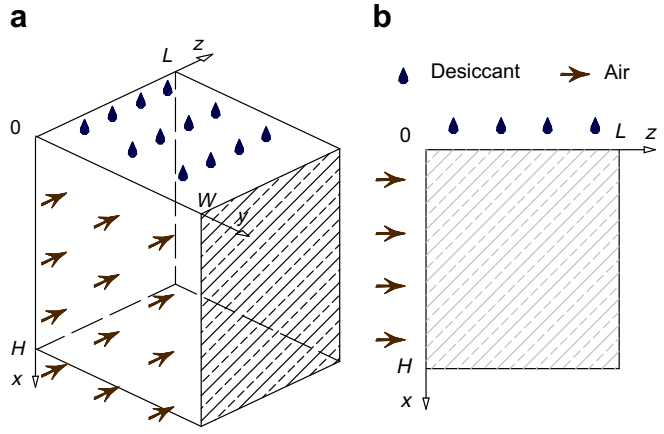

Fig. 1. Schematic of cross-flow packed bed dehumidifier: (a) three-dimensional view; and (b) sectional view.

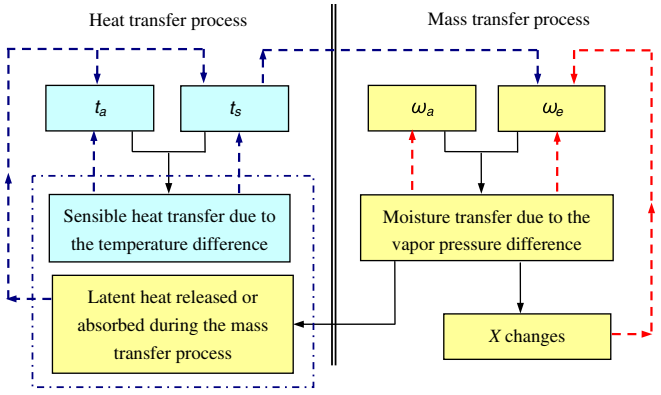

Fig. 2. Relationship between the heat transfer process and the mass transfer process in liquid desiccant packed bed dehumidifier.

$$\frac{\dot{m}_a}{H}\cdot\frac{\partial h_a}{\partial z}+\frac{\dot{m}_s}{L}\cdot\frac{\partial h_s}{\partial x}=0. \tag{9}$$

Desiccant enthalpy h_s can be expressed as [6]:

$$h_s=c_{p,s}(t_s-t_0)+\Delta h_s, \tag{10}$$

where $c_{p,s}$ is the specific heat of liquid desiccant, and Δh_s is the integral heat of solution at reference temperature t_0. As mentioned by Gandhidasan et al. [6], it can be assumed that the variation of Δh_s with desiccant concentration is neglected, when the desiccant concentration is almost unaltered. Desiccant enthalpy is almost linear with desiccant temperature when the desiccant concentration is constant, as shown in Fig. 3 for lithium bromide (LiBr) aqueous solution and lithium chloride (LiCl) aqueous solution. Based on Eq. (10) and Fig. 3, following relation can be gained: $dh_s=c_{p,s}dt_s$. Eq. (9) can then be rewritten as

$$m^*\cdot\frac{\partial h_a}{\partial z}+\frac{H}{L}\cdot\frac{\partial h_e}{\partial x}=0, \tag{11}$$

where m^* is the thermal capacity ratio of air to desiccant, as shown by Eq. (12). The equivalent air specific heat $c_{p,e}$ is defined by Eq. (13):

$$m^*=\frac{\dot{m}_a\cdot c_{p,e}}{\dot{m}_s\cdot c_{p,s}}, \tag{12}$$

$$c_{p,e}=\frac{dh_e}{dt_s}. \tag{13}$$

As predicted by Chung et al. [17], *Le* is equal one. Then Eq. (5) becomes:

$$\frac{\partial h_a}{\partial z}=-\frac{NTU}{L}\cdot(h_a-h_e). \tag{14}$$

The boundary conditions are

$$h_a=h_{a,in},\quad \omega_a=\omega_{a,in},\quad \text{at } z=0, \tag{15}$$

$$h_e=h_{e,in},\quad \omega_e=\omega_{e,in},\quad \text{at } x=0. \tag{16}$$

Combining Eqs. (11) and (14) and the boundary conditions, the analytical solutions of air enthalpy and desiccant equivalent enthalpy can be derived, which will be given in the next section.

3. Similarity between the cross-flow dehumidifier and cross-flow heat exchanger

The theoretical model of cross-flow heat exchanger is listed here to be compared with the cross-flow dehumidifier, since the flow pattern is the same. The schematic for cross-flow heat exchanger is shown in Fig. 4. The energy balance in the heat exchanger is shown as

$$\frac{c_{p,a}\cdot\dot{m}_a}{H}\cdot\frac{\partial t_a}{\partial z}+\frac{c_{p,s}\cdot\dot{m}_s}{L}\cdot\frac{\partial t_s}{\partial x}=0. \tag{17}$$

The above equation can be rewritten as Eq. (18), with the newly defined m_t^* shown in Eq. (19).

$$m_t^*\cdot\frac{\partial t_a}{\partial z}+\frac{H}{L}\cdot\frac{\partial t_s}{\partial x}=0, \tag{18}$$

$$m_t^*=\frac{\dot{m}_a\cdot c_{p,a}}{\dot{m}_s\cdot c_{p,s}}. \tag{19}$$

The heat transfer between the two fluids is shown by Eq. (20), with the newly defined NTU_t shown in Eq. (21).

$$\frac{\partial t_a}{\partial z}=-\frac{NTU_t}{L}\cdot(t_a-t_s), \tag{20}$$

$$NTU_t=\frac{\alpha\cdot A}{\dot{m}_a}. \tag{21}$$

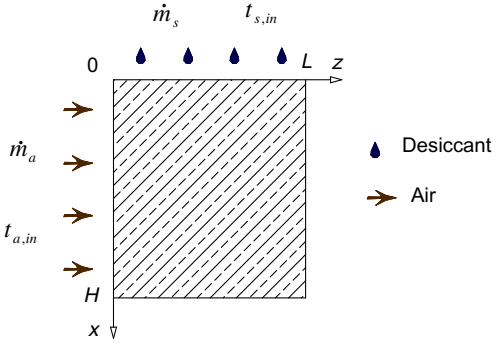

Fig. 4. Schematic of cross-flow heat exchanger.

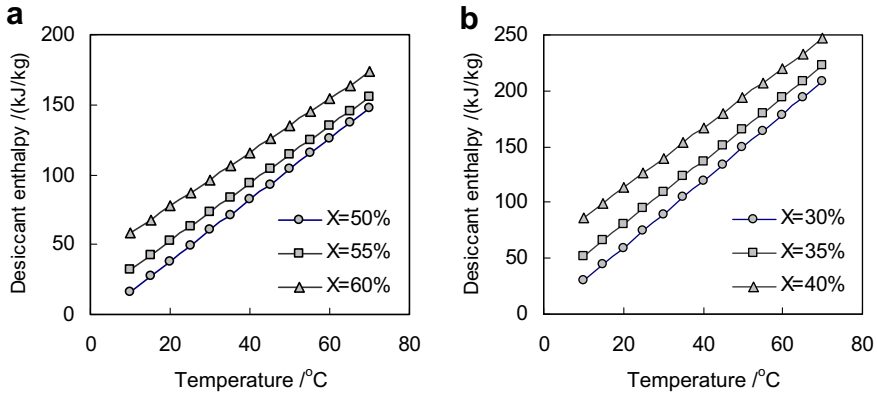

Fig. 3. Specific heat of liquid desiccant: (a) LiBr solution; and (b) LiCl solution.

Table 1
Comparison of the control equations for cross-flow dehumidifier and heat exchanger

	Dehumidifier	Heat exchanger
Control equations	Eq. (11): $m^* \cdot \frac{\partial h_a}{\partial z} + \frac{H}{L} \cdot \frac{\partial h_e}{\partial x} = 0$ Eq. (14): $\frac{\partial h_a}{\partial z} = \frac{\mathrm{NTU}}{L} \cdot (h_e - h_a)$	Eq. (18): $m_t^* \cdot \frac{\partial t_a}{\partial z} + \frac{H}{L} \cdot \frac{\partial t_s}{\partial x} = 0$ Eq. (20): $\frac{\partial t_a}{\partial z} = \frac{\mathrm{NTU}_t}{L} \cdot (t_s - t_a)$
Definitions	Eq. (12): $m^* = \frac{\dot{m}_a \cdot c_{p,e}}{\dot{m}_s \cdot c_{p,s}}$ Eq. (8): $\mathrm{NTU} = \frac{\alpha_m \cdot A}{\dot{m}_a}$	Eq. (19): $m_t^* = \frac{\dot{m}_a \cdot c_{p,a}}{\dot{m}_s \cdot c_{p,s}}$ Eq. (21): $\mathrm{NTU}_t = \frac{\alpha \cdot A}{\dot{m}_a}$
Inlet conditions	Eq. (15): $h_a = h_{a,in}$ at $z = 0$ Eq. (16): $h_e = h_{e,in}$ at $x = 0$	Eq. (22): $t_a = t_{a,in}$ at $z = 0$ Eq. (23): $t_s = t_{s,in}$ at $x = 0$

The inlet conditions of the two fluids are

$$t_a = t_{a,in} \quad \text{at } z = 0, \tag{22}$$

$$t_s = t_{s,in} \quad \text{at } x = 0. \tag{23}$$

The comparison of the control equations for the combined heat and mass transfer performance in cross-flow dehumidifier and heat transfer in cross-flow heat exchanger is shown in Table 1. The table indicates the forms of the control equations of the two processes are completely the same. Then, the solutions of Eqs. (11) and (14) for cross-flow dehumidifier can be derived by analogy with those of cross-flow heat exchanger.

4. Analytical solutions of the combined heat and mass transfer performance in cross-flow dehumidifier

4.1. Air enthalpy and desiccant equivalent enthalpy

The analytical solutions of air enthalpy and desiccant equivalent enthalpy in the cross-flow packed bed dehumidifier can be gained based on the available solutions for cross-flow heat exchanger. The detailed solving procedures are shown in reference [18,19], and only the analytical results for cross-flow dehumidifier are listed in present study. As suggested by Nusselt [18,19], several dimensionless parameters are defined as follows for convenience:

$$\xi = \frac{z}{L}, \quad \eta = \frac{x}{H},$$
$$\varsigma_a = \frac{h_a - h_{e,in}}{h_{a,in} - h_{e,in}}, \quad \varsigma_e = \frac{h_e - h_{e,in}}{h_{a,in} - h_{e,in}}, \tag{24}$$
$$p = \mathrm{NTU}, \quad q = \mathrm{NTU} \cdot m^*.$$

The analytical solution of air dimensionless enthalpy $\varsigma_a(\xi,\eta)$ is shown as follows:

$$\varsigma_a(\xi,\eta) = \phi_0(\xi,\eta) + \phi_1(\xi,\eta) + \phi_2(\xi,\eta) + \cdots + \phi_n(\xi,\eta) + \cdots, \tag{25}$$

where

$$\phi_0(\xi,\eta) = \mathrm{e}^{-p\xi},$$
$$\phi_1(\xi,\eta) = p\xi \cdot \mathrm{e}^{-p\xi} \cdot (1 - \mathrm{e}^{-q\eta}),$$
$$\cdots$$
$$\phi_n(\xi,\eta) = \frac{1}{n!} \cdot p^n \xi^n \cdot \mathrm{e}^{-p\xi} \cdot \left[1 - \mathrm{e}^{-q\eta} - q\eta \cdot \mathrm{e}^{-q\eta} - \cdots - \frac{1}{(n-1)!} q^{n-1} \eta^{n-1} \cdot \mathrm{e}^{-q\eta}\right].$$

Desiccant dimensionless equivalent enthalpy $\varsigma_e(\xi,\eta)$ is shown as

$$\varsigma_e(\xi,\eta) = \Pi_0(\xi,\eta) + \Pi_1(\xi,\eta) + \Pi_2(\xi,\eta) + \cdots + \Pi_n(\xi,\eta) + \cdots, \tag{26}$$

where

$$\Pi_0 = \mathrm{e}^{-(p\xi+q\eta)} \cdot (\mathrm{e}^{q\eta} - 1),$$
$$\Pi_1 = p\xi \cdot \mathrm{e}^{-(p\xi+q\eta)} \cdot (\mathrm{e}^{q\eta} - 1 - q\eta),$$
$$\cdots$$
$$\Pi_n = \frac{1}{n!} p^n \xi^n \cdot \mathrm{e}^{-(p\xi+q\eta)} \cdot \left[\mathrm{e}^{q\eta} - 1 - q\eta - \frac{q^2\eta^2}{2} - \frac{q^n\eta^n}{n!}\right].$$

4.2. Air humidity ratio and desiccant equivalent humidity ratio

The relationship of desiccant h_e and ω_e at constant concentration is shown in Fig. 5, with the desiccant temperature

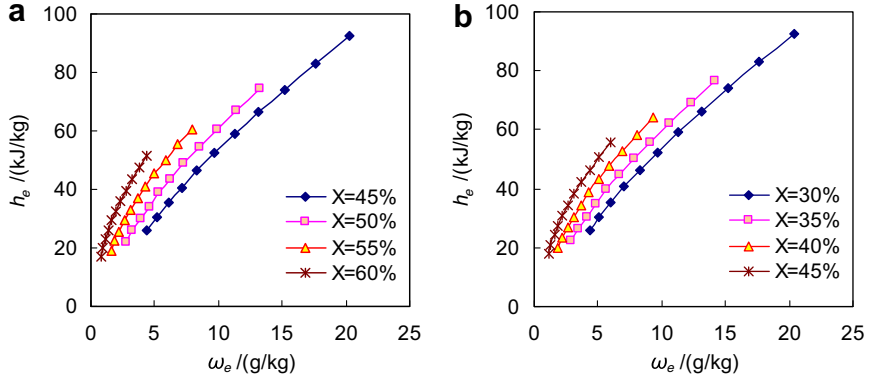

Fig. 5. Relationship of desiccant equivalent enthalpy and equivalent humidity ratio: (a) LiBr solution; and (b) LiCl solution.

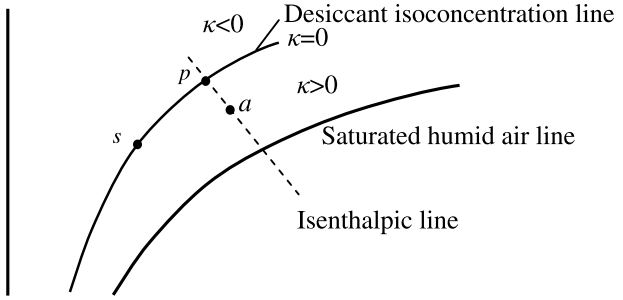

Fig. 6. Air and desiccant inlet status shown in psychrometic chart.

range of 15–40 °C. As indicated by the figure, following equation can be assumed at desiccant isoconcentration line:

$$h_e = c_1\omega_e + c_2. \tag{27}$$

Fig. 6 shows air and desiccant inlet status, denoted as a and s, respectively, where p is the intersection point of inlet desiccant isoconcentration line and inlet air isenthalpic line. The humidity ratio of point p is ω^*, which equals to $\omega_{a,in}$ when inlet air is at inlet desiccant isoconcentration line. According to Eq. (27), air inlet enthalpy and desiccant inlet equivalent enthalpy can be expressed as

$$h_{a,in} = c_1\omega^* + c_2, \tag{28}$$

$$h_{e,in} = c_1\omega_{e,in} + c_2. \tag{29}$$

Air and desiccant dimensional humidity ratios are defined as

$$\gamma_a = \frac{\omega_a - \omega_{e,in}}{\omega^* - \omega_{e,in}}, \quad \gamma_e = \frac{\omega_e - \omega_{e,in}}{\omega^* - \omega_{e,in}}. \tag{30}$$

Substitute Eqs. (27)–(29) into Eq. (24) to gain:

$$\varsigma_e = \frac{h_e - h_{e,in}}{h_{a,in} - h_{e,in}} = \frac{\omega_e - \omega_{e,in}}{\omega^* - \omega_{e,in}} = \gamma_e. \tag{31}$$

Therefore, the analytical solution of desiccant dimensionless equivalent humidity ratio is the same with that of dimensionless equivalent enthalpy. The solving procedure of air humidity ratio is similar with that of air enthalpy, and the final results are

$$\gamma_a(\xi,\eta) = \varsigma_a(\xi,\eta) + \frac{1}{1-\kappa}e^{-p\xi}, \tag{32}$$

where κ is the difference between air inlet parameter and the desiccant inlet isoconcentraion line, as calculated by

$$\kappa = \frac{\omega_{a,in} - \omega^*}{\omega_{a,in} - \omega_{e,in}}. \tag{33}$$

Air temperature can then be calculated with the known enthalpy and humidity ratio.

4.3. Enthalpy efficiency and moisture efficiency

Enthalpy efficiency ε_h and moisture efficiency ε_m are used to predict the dehumidifier performance, which are defined as the variance of air enthalpy or humidity ratio through the dehumidifier to the maximal variance, as shown by Eqs. (34) and (35), respectively.

$$\varepsilon_h = \frac{h_{a,in} - h_{a,out}}{h_{a,in} - h_{e,in}} \times 100\%, \tag{34}$$

$$\varepsilon_m = \frac{\omega_{a,in} - \omega_{a,out}}{\omega_{a,in} - \omega_{e,in}} \times 100\%. \tag{35}$$

Substitute Eq. (25) into Eq. (34) to gain the enthalpy efficiency:

$$\varepsilon_h = 1 - (\psi_0 + \psi_1 + \psi_2 + \cdots + \psi_n + \cdots), \tag{36}$$

where

$$\psi_0 = e^{-p},$$

$$\psi_1 = p\psi_0 + \frac{p}{q}\cdot e^{-p}\cdot(e^{-q} - 1),$$

$$\psi_2 = \frac{p}{2}(2\psi_1 - p\psi_0) + \frac{p^2}{2}\cdot e^{-(p+q)},$$

$$\cdots$$

$$\psi_n = \frac{p}{n}\left(2\psi_{n-1} - \frac{p}{n-1}\psi_{n-2}\right) + \frac{p^n}{n!}\cdot\frac{q^{n-2}}{(n-1)!}\cdot e^{-(p+q)}.$$

Combine Eqs. (32), (35) and (36) to yield:

$$\varepsilon_m = \varepsilon_h + \kappa\cdot(1 - \varepsilon_h - e^{-NTU}). \tag{37}$$

As predicted by Eqs. (36) and (37), enthalpy efficiency ε_h is the function of m^* and NTU, and moisture efficiency ε_m is the function of m^*, NTU and κ. The value of κ is determined by the air and desiccant inlet parameters, as shown

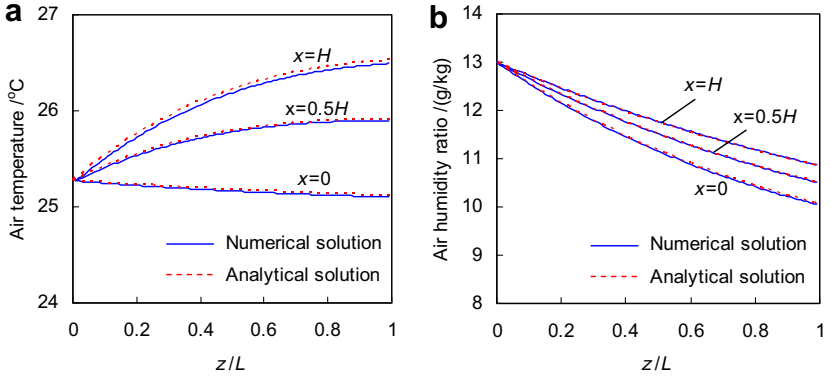

Fig. 7. Comparison of analytical solutions and numerical results: (a) air temperature; and (b) air humidity ratio.

by Fig. 6, $\kappa = 0$ when air inlet parameter is located in desiccant inlet isoconcentration line. Moisture efficiency ε_m is equal to ε_h when $\kappa = 0$; and greater than ε_h when $\kappa > 0$, that is air inlet parameter is in the right side of the desiccant inlet isoconcentration line; and lower than ε_h when $\kappa < 0$.

5. Validation of the analytical solutions

5.1. Comparison with numerical results

The distributions of air parameters within the cross-flow dehumidifier by numerical simulation as well as analytical results are shown in Fig. 7. LiBr aqueous solution is used as liquid desiccant, m^* and NTU are both equal one. Air inlet parameters are 30 °C, 18 g/kg, and desiccant inlet parameters are 25 °C, 45% concentration.

In the numerical simulation [10], the assumption of constant desiccant flow rate is not adopted. Based on the comparison results, analytical solutions accord well with the numerical results, which can be directly used to analyze the field distributions within the cross-flow dehumidifier.

5.2. Comparison with experimental results

In the dehumidification experiments, LiBr aqueous solution is chosen as liquid desiccant, and Celdek 7090 structured packing is taken as packing material. The detailed experimental test was described in an earlier paper [16]. Two dehumidification experiments with different dehumidifier sizes are used to validate the analytical solutions, the dehumidifier sizes and air and desiccant inlet parameters are shown in Tables 2 and 3, respectively.

Enthalpy and moisture efficiencies comparison results between the analytical and experimental results are shown in Fig. 8, almost all the discrepancies are within ±20%. For experiment A (sizes of $0.55 \times 0.4 \times 0.35\ m^3$), the average absolute differences are 6.3% and 5.6% for enthalpy efficiency and moisture efficiency respectively. For experiment B (sizes of $0.55 \times 0.3 \times 0.35\ m^3$), the average absolute difference are 8.0% and 2.1% for enthalpy efficiency and moisture efficiency respectively. Thus, the analytical solutions of the heat and mass transfer efficiencies accord well with the experimental findings, which can be used to predict the combined heat and mass transfer performance in the dehumidifier.

Table 2
Parameters of experimental cross-flow packed bed dehumidifiers

	Sizes of dehumidifier/m			m^*	NTU	ε_h (%)	ε_m (%)
	H	L	W				
Module A	0.55	0.40	0.35	0.55–1.65	0.67–1.57	28.4–65.4	37.8–68.1
Module B	0.55	0.30	0.35	0.51–2.58	0.37–0.84	23.1–53.1	24.0–49.7

Table 3
Desiccant and air inlet parameters during the dehumidification experiments

	Air inlet parameters			Desiccant inlet parameters		
	$\dot{m}_a$ (kg/s)	t_a (°C)	ω_a (kg/kg)	$\dot{m}_s$ (kg/s)	t_s (°C)	X (%)
Module A	0.30–0.47	24.7–33.9	0.010–0.021	0.30–0.64	20.1–29.5	42.6–54.8
Module B	0.34–0.48	25.4–35.4	0.010–0.018	0.21–0.56	19.7–27.2	42.2–54.1

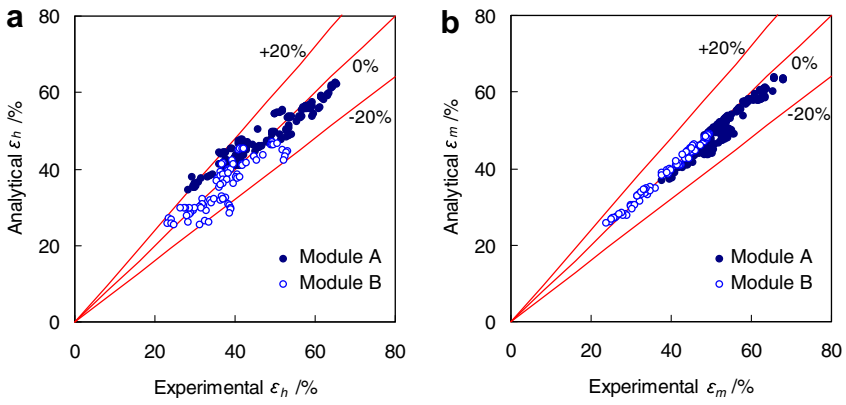

Fig. 8. Comparison of analytical solutions and experimental findings: (a) enthalpy efficiency; and (b) moisture efficiency.

6. Utilization of the analytical solutions

6.1. Main performance factors

The dimensionless parameter κ is constant, once the processed parameters are determined. The main variables that influences the dehumidifier effectiveness are m^* and NTU. Fig. 9 shows the effect of m^* and NTU on the enthalpy and moisture efficiencies of the cross-flow dehumidifier. When the heat capacity ratio m^* is constant, the dehumidifier efficiencies increase with the increase of NTU. However, continuing increase NTU will contribute little on the dehumidifier efficiencies, when NTU arrives at a large value.

As indicated by Eq. (8), NTU is the function of mass transfer coefficient α_m, total mass transfer area A and air flow rate $\dot{m}_a$. The overall mass transfer area A can be expressed as Eq. (38) when the packing is fully wet:

$$A = a \cdot V, \tag{38}$$

where, a is the specific area of packing material, and V is the volume of the packing material in the dehumidifier. Choosing the packing material with large specific area or increasing the packing volume can benefit on increasing NTU, yet they will increase the initial cost of the dehumidifier.

The relation of NTU and dimensionless mass transfer coefficient Sh is given by Eq. (39), where d_e is the equivalent size of the packing, ρ_a and D_a is the density and diffusion coefficient of air.

$$Sh = \mathrm{NTU} \cdot \frac{\dot{m}_a \cdot d_e}{\rho_a \cdot D_a \cdot a \cdot V}. \tag{39}$$

For the liquid desiccant dehumidification process, Sh correlation [20] can be correlated by Eq. (40). In the experiments of present cross-flow dehumidification, c_1–c_4 are 1.363, 0.333, 0.396 and 1.913, respectively:

$$Sh_a = c_0 (Re_a)^{c_1} (Sc_a)^{c_2} \left(\frac{F_s}{F_a}\right)^{c_3} \left(1 - \frac{X}{100}\right)^{c_4}. \tag{40}$$

Both heat and mass transfer performance and pressure drop should be considered in the optimization of the dehumidifier, the former performance affects the overall efficiency of the entire liquid desiccant system, and the latter one is the key factor on the energy consumption of the blower.

The changes of pressure drop per unit thickness Δp^* with air and desiccant flow rate is shown in Fig. 10. As indicated by the figure, air flow rate F_a (or air surface velocity v_a) has strong effect on Δp^*, while desiccant flow rate F_s provides little influence. In simplification, Δp^* is expressed as

$$\Delta p^* = -35.7 + 58.4 \cdot v_a + 41.5 \cdot v_a^2. \tag{41}$$

Therefore, the pressure drop Δp can be calculated by $\Delta p = \Delta p^* \cdot L$.

6.2. Optimization of the cross-flow dehumidifier

The optimization analysis is to decrease the pressure drop and improve the heat and mass transfer performances by minimize initial cost (packing volume). In other

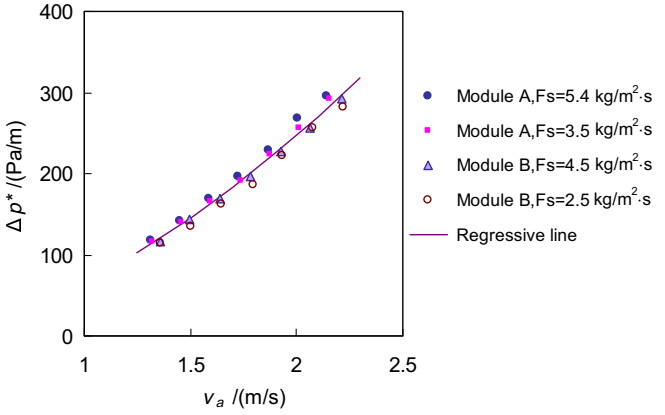

Fig. 10. Pressure drop of the experimental cross-flow packed bed dehumidifier.

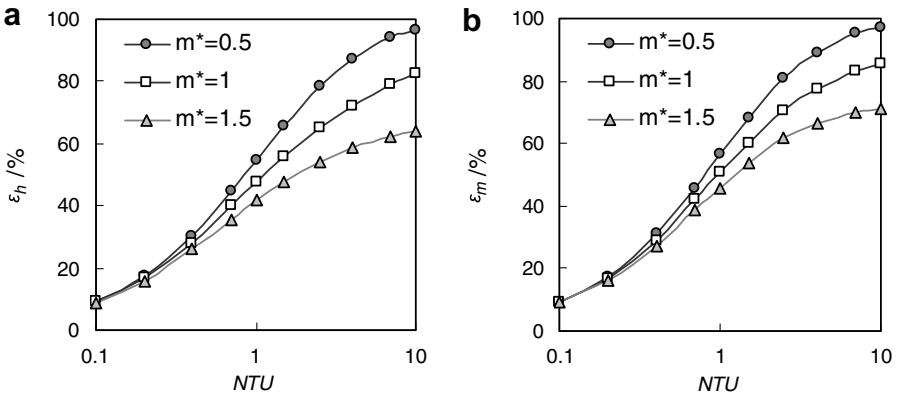

Fig. 9. Effect of m^* and NTU on the dehumidifier effectiveness: (a) enthalpy efficiency; and (b) moisture efficiency.

words, to realize the same heat and mass transfer performance and pressure drop, with as less as possible packing volume.

For the designed processed air flow rate, the values of m^* and NTU can be expressed by Eqs. (42) and (43), respectively, if the desiccant flow rate, packing volume or its distribution in different dimensions are changed. Where the subscript 0 stands for the original status, and $\dot{m}_a = \dot{m}_{a,0}$:

$$\frac{m^*}{m_0^*} = \left(\frac{\dot{m}_s}{\dot{m}_{s,0}}\right)^{-1}, \tag{42}$$

$$\frac{\mathrm{NTU}}{\mathrm{NTU}_0} = \left(\frac{\dot{m}_s}{\dot{m}_{s,0}}\right)^{c_3} \cdot \left(\frac{V}{V_0}\right)^{1-c_1} \left(\frac{L}{L_0}\right)^{c_1-c_3} \left(\frac{H}{H_0}\right)^{c_3}. \tag{43}$$

As seen from Fig. 9, enthalpy and moisture efficiencies increase with increasing NTU and decreasing m^*. The heat and mass transfer performances of the dehumidifier can be predicted when the desiccant flow rate or the packing volume changes, through Eqs. (42) and (43) and the derived analytical solutions.

The sizes of a cross-flow dehumidification module applied in a liquid desiccant based outdoor air processor [21] are $0.5 \times 0.5 \times 1.2\ \mathrm{m}^3$ for the designed air flow rate of $3600\ \mathrm{m}^3/\mathrm{h}$. The performance of the module is shown in Table 4, which is denoted as "original module". The typical air inlet parameters are 30 °C and 15 g/kg, and desiccant inlet parameters are 25 °C, 48% concentration and flow rate of 4.5 t/h. The packing and liquid desiccant used in the module is the same with the experimental test.

Table 4
Performance of the cross-flow packed bed dehumidifiers with different sizes

	$H \times L \times W$ (m^3)	$\frac{V}{V_0}$	$\frac{\dot{m}_s}{\dot{m}_{s,0}}$	ε_h (%)	ε_m (%)	Δp (Pa)
Original module	0.5 × 0.5 × 1.2	1	1	49.3	54.0	88.5
Optimized module	0.6 × 0.4 × 0.83	0.67	1	49.3	54.1	98.8
	0.6 × 0.35 × 0.83	0.58	1.1	49.7	53.9	86.5

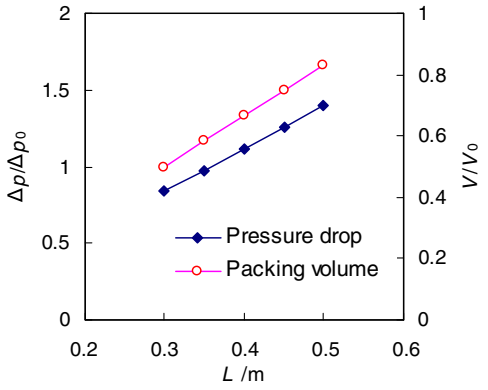

Fig. 12. Effect of dehumidifier sizes on the pressure drop and packing volume of the dehumidifier.

In the optimization of the dehumidification module, air surface velocity is chosen as 2 m/s in consideration of decreasing packing volume, pressure drop and avoid of desiccant carry-over by the air stream, and hence $H \times W = 0.5\ \mathrm{m}^2$ according to the designed air flow rate. Fig. 11 shows the effect of dehumidifier height (H), thickness (L) and desiccant flow rate on the dehumidifier performance. Increasing dehumidifier height or thickness, or desiccant flow rate can improve the heat and mass transfer performance. The effects of dehumidifier sizes on pressure drop and packing volume are shown in Fig. 12. The smaller the thickness L is, the smaller pressure drop and smaller packing volume are. Hence, smaller dehumidifier thickness is recommended in considering the pressure drop and packing volume. Table 4 gives the possible optimized dehumidifier sizes, considering the height restrict in some applications. In the end, the optimized sizes of $0.6 \times 0.35 \times 0.83\ \mathrm{m}^3$ are selected, with the desiccant flow rate of 10% higher than the original module. The heat and mass transfer performances and the pressure drop of the optimized module are about the same with the original module, yet the volume is only 58% compared with the original module.

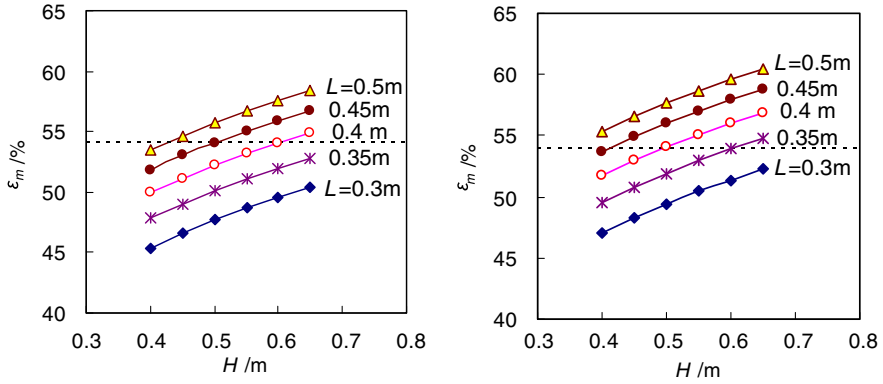

Fig. 11. Effect of dehumidifier sizes on the heat and mass transfer performance of cross-flow dehumidifier with different desiccant flow rate: (a) $\dot{m}_s = \dot{m}_{s,0}$; and (b) $\dot{m}_s = 1.1 \times \dot{m}_{s,0}$.

7. Conclusions

The analytical solutions of the combined heat and mass transfer performance in the cross-flow packed bed dehumidifier are given in the present study, based on the similarity between the combined heat and mass transfer processes in cross-flow dehumidifier and the heat transfer process in cross-flow heat exchanger.

The distributions of air and desiccant parameters within the cross-flow dehumidifier by analytical solutions, accord well with the numerical simulations results. And the analytical solutions of enthalpy and moisture efficiencies, accord well with the corresponding experimental findings, and the average absolute differences are both within 8%.

The analytical solutions can be used to predict the combined heat and mass transfer performance of cross-flow dehumidifier under different operating conditions, and instruct the optimization of the dehumidifier. For the design air flow rate of 3600 m^3/h, the dehumidifier sizes before and after optimization are $0.5 \times 0.5 \times 1.2\ m^3$ and $0.6 \times 0.35 \times 0.83\ m^3$, respectively. Compared to the original module sizes, the optimized packing volume decreases to 58%, the enthalpy and moisture efficiencies and the packing pressure drop are almost the same.

Acknowledgements

The research described in this manuscript was supported by Specialized Research Fund for the Doctoral Program of Higher Education in China (No. 20050003051) and National Natural Science Foundation of China (No. 50778094).

References

[1] D.G. Waugaman, A. Kini, C.F. Kettleborough, A review of desiccant cooling systems, J. Energy Resour. Technol. 115 (1993) 1–8.
[2] S. Jain, P.L. Dhar, S.C. Kaushik, Evaluation of liquid desiccant based evaporative cooling cycles for typical hot and humid climates, Heat Recov. Syst. CHP 14 (1994) 621–632.
[3] V. Oberg, D.Y. Goswami, Experimental study of the heat and mass transfer in a packed bed liquid desiccant air dehumidifier, J. Sol. Energy Eng. 120 (1998) 289–297.
[4] H.M. Factor, G. Grossman, A packed bed dehumidifier/regenerator for solar air conditioning with liquid desiccants, Sol. Energy 24 (1980) 541–550.
[5] P. Gandhidasan, C.F. Kettleborough, M.R. Ullah, Calculation of heat and mass transfer coefficients in a packed tower operating with a desiccant–air contact system, J. Sol. Energy Eng. 108 (1986) 123–128.
[6] P. Gandhidasan, M.R. Ullah, C.F. Kettleborough, Analysis of heat and mass transfer between a desiccant–air system in a packed tower, J. Sol. Energy Eng. 109 (1987) 89–93.
[7] D.I. Stevens, J.E. Braun, S.A. Klein, An effectiveness model of liquid desiccant system heat/mass exchangers, Sol. Energy 42 (1989) 449–455.
[8] J.A. Rocha, J.L. Bravo, J.R. Fair, Distillation columns containing structured packings: a comprehensive model for their performance. 2. mass-transfer model, Ind. Eng. Chem. Res. 35 (1996) 1660–1667.
[9] Z.F. Lu, P.L. Chen, X. Zhang, Approximate analytical solution of heat and mass transfer processes in packed-type cross-flow liquid desiccant system and its experimental verification, J. Tongji Univ. 29 (2001) 149–153 (in Chinese).
[10] X.H. Liu, Y. Jiang, K.Y. Qu, Heat and mass transfer model of cross-flow liquid desiccant air dehumidifier/regenerator, Energy Conv. Manage. 48 (2007) 546–554.
[11] Y.J. Dai, H.F. Zhang, Numerical simulation and theoretical analysis of heat and mass transfer in a cross flow liquid desiccant air dehumidifier packed with honeycomb paper, Energy Conv. Manage. 45 (2004) 1343–1356.
[12] A. Ali, K. Vafai, A.R.A. Khaled, Comparative study between parallel and counter flow configurations between air and falling film desiccant in the presence of nanoparticle suspensions, Int. J. Energy Res. 27 (2003) 725–745.
[13] A. Ali, K. Vafai, A.R.A. Khaled, Analysis of heat and mass transfer between air and falling film in a cross flow configuration, Int. J. Heat Mass Transfer 47 (2004) 743–755.
[14] N. Fumo, D.Y. Goswami, Study of an aqueous lithium chloride desiccant system: air dehumidification and desiccant regeneration, Sol. Energy 72 (2002) 351–361.
[15] T.W. Chung, H. Wu, Mass transfer correlation for dehumidification of air in a packed absorber with an inverse U-shaped tunnel, Sep. Sci. Technol. 35 (2000) 1502–1514.
[16] X.H. Liu, Y. Zhang, K.Y. Qu, Y. Jiang, Experimental study on mass transfer performance of cross-flow dehumidifier using liquid desiccant, Energy Conv. Manage. 47 (2006) 2682–2692.
[17] T.W. Chung, H. Wu, Comparison between spray towers with and without fin coils for air dehumidification using triethylene glycol solutions and development of the mass-transfer correlations, Ind. Eng. Chem. Res. 39 (2000) 2076–2084.
[18] W. Nusselt, Der Warmeubergang im Kreuzstrom, Zeitschrift des Vereines Deutscher Ingenieure 55 (1911) 2021–2024.
[19] W. Nusselt, Eine neue Formel fur den Warmedurchgang im Kreuzstrom, Technische Meahanik und Thermodynamik 1 (1930) 417–422.
[20] T.W. Chung, T.K. Ghosh, A.L. Hines, D. Novosel, Dehumidification of moist air with simultaneous removal of selected indoor pollutants by triethylene glycol solutions in a packed-bed absorber, Sep. Sci. Technol. 30 (1995) 1809–1832.
[21] Z. Li, X.H. Liu, Y. Jiang, X.Y. Chen, New type of fresh air processor with liquid desiccant total heat recovery, Energy Build. 37 (2005) 587–593.